Formation, crystal structure and co-ordination chemistry of the [Mn^{III}(oespz)(SH)] [oespz^{2-} = 2,3,7,8,12,13,17,18-octakis(ethyl-sulfanyl)-5,10,15,20-tetraazaporphyrinate dianion] complex

Giampaolo Ricciardi,[a] Alessandro Bencini,[b] Sandra Belviso,[a] Alfonso Bavoso[a] and Francesco Lelj *,[a]

[a] *Dipartimento di Chimica, Università della Basilicata, Via N. Sauro 85, 85100 Potenza, Italy*
[b] *Dipartimento di Chimica, Università di Firenze, Via Maragliano 77, 50144 Firenze, Italy*

Reaction of [Mn(oespz)] [oespz^{2-} = 2,3,7,8,12,13,17,18-octakis(ethylsulfanyl)-5,10,15,20-tetraazaporphyrinate dianion (porphyrazinate)] with CS$_2$ and, subsequently, with THF, afforded the hydrogensulfido(1−)manganese(III) ethylsulfanylporphyrazinate [Mn(oespz)(SH)], in high yield. The S–H stretching absorptions are not observed in the IR spectrum of the complex, whereas a peak at δ 10.3 (*vs.* SiMe$_4$) ascribed to the hydrogensulfido proton resonance, is observed in the ^{1}H NMR spectrum. The complex was shown to be isostructural with [M(oespz)Cl] (M = Fe or Mn) by X-ray crystallography. The crystal packing of the complex consists of slipped stacks of dimeric units with the monomers positioned in a *trans* fashion with respect to the Mn−S$_{apical}$ bond. Magnetic data are consistent with weakly antiferromagnetically coupled high spin (*S* = 2) manganese(III) centers. A possible pathway to the oxidative addition of CS$_2$ to the manganese(II) center has been proposed. In CHCl$_3$ [Mn(oespz)(SH)] reacts reversibly through the axial hydrosulfido ligand with the sterically hindered base 2,4,6-trimethylpyridine, whereas the complex co-ordinates 1-methylimidazole reversibly on the vacant site of manganese. Treatment of the complex with 1-methylimidazole in benzene leads to a Mn^{III}–Mn^{II} redox process, as deduced from the UV/VIS spectra.

The recently synthesized complex [Mn(oespz)] [oespz = 2,3,7,8,12,13,17,18-octakis(ethylsulfanyl)-5,10,15,20-tetraaza-porphyrinate (porphyrazinate)] possesses, compared to the congener Mn^{II}–tetrapyrroles, an unusually nucleophilic metallic center.[1,2] The easy abstraction of halogen atoms from halogenated hydrocarbons by [Mn(oespz)], *via* oxidative addition of the halogen to manganese, represents a clear example of how this feature may work.[2,3] While exploring the reactivity of [Mn(oespz)] towards weak electrophiles we have found that it reacts with carbon disulfide to afford the hydrogensulfido derivative [Mn(oespz)(SH)]. This reaction seemed intriguing to us. Although, for instance, CS$_2$ has a widely studied organometallic chemistry[4] and, upon electrochemical or chemical reduction (normally by alkaline-earth metals in DMF) becomes the basic building block of 1,3-dithiol-2-thione-4,5-dithiolate (dmit),[5] or ethylenetetrathiolate (ett),[6] ligands, direct reaction of a Mn^{II}–tetrapyrrole complex with carbon disulfide is unprecedented. In addition, the chemistry of SH$^-$ containing complexes could be relevant to metal sulfide hydrosulfurization catalysts[7] and transition-metal tetrapyrroles with a hydrosulfido axial ligand are well suited to mimic the spectral properties of cytochrome P-450 and chloroperoxidase.[8] Moreover mono- and poly-nuclear Mn^{III} is of central importance in biological systems such as superoxide dismutase[9] and catalase,[10] while Mn^{III} porphyrins[11] and phthalocyanines (pc)[12] have been used as building blocks in the construction of molecule-based magnets.

Thus we decided to investigate the reaction of [Mn(oespz)] with CS$_2$ and the physicochemical properties of the resulting complex, [Mn(oespz)(SH)]. This paper reports the synthesis, structural characterization and magnetic properties of [Mn(oespz)(SH)]. The co-ordinating capability of the complex towards strong σ-donors such as 1-methylimidazole (1-mim) as well as toward sterically hindered organic bases such as 2,4,6-trimethylpyridine is also explored with the aim of elucidating the structure of the complex in solution and the possible effects of the sixth ligand on the electronic structure of the complex.

Experimental

Materials

All chemicals and solvents (Aldrich Chemicals Ltd.) were of reagent grade and used in the syntheses as supplied. Solvents used in physical measurements were of spectroscopic or HPLC grade. The compound [Mn(O$_2$CMe)$_2$] was obtained from Strem. Anhydrous ethanol, tetrahydrofuran (THF) and dimethylformamide (DMF) were obtained according to the procedures described in the literature.[13] Silica gel used for chromatography was Merck Kiselgel 60 (270–400 mesh). Dichloromethane for voltammetric studies was refluxed under nitrogen with CaH$_2$ for at least 48 h and stored over 4 Å molecular sieves. The salt [NBu$^n_4$][BF$_4$] was recrystallized from ethanol and dried under partial vacuum. Air- and moisture-sensitive chemicals were handled under an inert nitrogen atmosphere using standard Schlenk techniques or in a glove box. Carbon disulfide was purged of H$_2$S and H$_2$O contaminants by reaction with lead acetate [typically CS$_2$ (100.0 cm^3) was shaken with lead acetate (0.1 g) under N$_2$ for 24 h] and subsequent distillation from CaH$_2$.

Physical measurements

Microanalyses were performed by the Analytische Laboratorien of Professor H. Malissa and G. Reuter Gmbh, Gummersbach, Germany and by the Butterworth Laboratories Ltd, Teddington, UK. Infrared spectra were run as KBr disks on a 5PC Nicolet FT-IR spectrometer over the range 400–4000 cm^{-1}. Fast-atom bombardment mass spectra (FAB MS) were recorded on a VG ZAB 2SE double focusing mass spectrometer equipped with a caesium gun operating at 25 kV (2 mA) using a 3-nitrobenzyl alcohol (NBA) matrix. Solution electronic spectra in 1 or 10 cm path length quartz cells or on thin film in the region 200–2500 nm were performed on a UV-VIS-NIR 05E Cary spectrophotometer. Thin films for electronic spectroscopy studies were built by spreading, under a N$_2$ stream, 1.0 cm^3 of a 1.0 × 10^{-5} M degassed sample solution in CHCl$_3$, on a quartz

Table 1 Data collection and refinement parameters for [Mn(oespz)-(SH)]

Formula	$C_{32}H_{41}MnN_8S_9$
M	881.29
Crystal system	Monoclinic
Space group	$P2_1/c$
λ(Cu-Kα)/Å	1.541 84
a/Å	15.876(4)
b/Å	17.932(4)
c/Å	15.642(3)
β/°	117.61(2)
U/Å^3	3946.0(1)
Z	4
D_c/g cm^{-3}	1.48
μ/cm^{-1}	74.3
T/K	298
$F(000)$	1828
Crystal size/mm	$0.18 \times 0.39 \times 0.51$
2θ Range/°	1–69
h, k, l Ranges	-19 to 19, 0–21, 0–21
Unique reflections	7474
Observed reflections [$I > 3\sigma(I)$]	3631
Goodness of fit	2.64
No. parameters	451
Maximum Δ/σ	0.2
Maximum, minimum $\Delta\rho$/e Å^{-3}	0.481, -0.09
R^a	0.051
$R'^{\,b}$	0.053

^{a} $R = \Sigma(\|F_o| - |F_c\|)/\Sigma|F_o|$. ^{b} $R' = [\Sigma w(\|F_o| - |F_c\|)^2/\Sigma w|F_o|^2]^{\frac{1}{2}}$.

Table 2 Selected bond lengths (Å) and angles (°) with estimated standard deviations in parentheses for [Mn(oespz)(SH)]

Mn–S$_{apical}$	2.374(3)	N(5)–C(4)	1.328(7)
Mn–N(1)	1.949(5)	N(5)–C(5)	1.340(8)
Mn–N(2)	1.938(4)	N(6)–C(8)	1.319(8)
Mn–N(3)	1.955(5)	N(6)–C(9)	1.305(7)
Mn–N(4)	1.945(4)	N(7)–C(12)	1.323(7)
S(1)–C(2)	1.751(7)	N(7)–C(13)	1.326(9)
S(2)–C(3)	1.717(6)	N(8)–C(1)	1.320(7)
S(3)–C(6)	1.727(6)	N(8)–C(16)	1.328(8)
S(4)–C(7)	1.723(6)	C(1)–C(2)	1.436(9)
S(5)–C(10)	1.725(6)	C(2)–C(3)	1.368(7)
S(6)–C(11)	1.738(6)	C(3)–C(4)	1.471(9)
S(7)–C(14)	1.727(6)	C(5)–C(6)	1.438(8)
S(8)–C(15)	1.724(7)	C(6)–C(7)	1.377(9)
N(1)–C(1)	1.373(7)	C(7)–C(8)	1.435(7)
N(1)–C(4)	1.361(7)	C(9)–C(10)	1.464(8)
N(2)–C(5)	1.371(7)	C(10)–C(11)	1.370(7)
N(2)–C(8)	1.392(8)	C(11)–C(12)	1.459(9)
N(3)–C(9)	1.370(7)	C(13)–C(14)	1.447(8)
N(3)–C(12)	1.362(7)	C(14)–C(15)	1.365(9)
N(4)–C(13)	1.380(7)	C(15)–C(16)	1.440(7)
N(4)–C(16)	1.377(8)	C(17)–C(18)	1.51(1)
S$_{apical}$–Mn–N(1)	100.6(2)	N(1)–C(1)–C(2)	109.3(4)
S$_{apical}$–Mn–N(2)	100.1(2)	N(2)–C(5)–C(6)	111.4(5)
S$_{apical}$–Mn–N(3)	96.6(2)	N(3)–C(9)–C(10)	109.1(4)
S$_{apical}$–Mn–N(4)	96.9(2)	N(4)–C(13)–C(14)	110.2(6)
N(1)–Mn–N(2)	88.8(2)	C(1)–C(2)–C(3)	108.5(5)
N(1)–Mn–N(4)	88.4(2)	C(5)–C(6)–C(7)	105.6(5)
N(2)–Mn–N(3)	88.9(2)	C(9)–C(10)–C(11)	107.0(5)
N(3)–Mn–N(4)	88.7(2)	C(13)–C(14)–C(15)	105.7(5)
C(1)–N(1)–C(4)	107.1(5)	S(1)–C(2)–C(3)	127.7(5)
C(5)–N(2)–C(8)	105.6(4)	S(2)–C(3)–C(2)	137.4(5)
C(9)–N(3)–C(12)	107.6(5)	S(3)–C(6)–C(7)	124.1(5)
C(13)–N(4)–C(16)	106.6(4)	S(4)–C(7)–C(6)	122.0(4)
C(4)–N(5)–C(5)	121.9(5)	S(5)–C(10)–C(11)	137.1(5)
C(8)–N(6)–C(9)	123.2(5)	S(6)–C(11)–C(10)	130.2(5)
C(12)–N(7)–C(13)	122.2(5)	S(7)–C(14)–C(15)	126.7(5)
C(1)–N(8)–C(16)	122.9(5)	S(8)–C(15)–C(14)	122.8(4)

slide (Corning, $1.0 \times 3.0 \times 0.1$ cm). Cuvettes for spectroscopic titrations were filled in a glove box under N$_2$ and the titrant was added with the help of a microsyringe. Proton NMR spectra were performed on a Bruker AM 300 MHz spectrometer.

Polycrystalline powder EPR spectra were measured in the temperature range 4.2–300 K using a Varian E-9 spectrometer. Liquid-helium temperature was reached with an ESR90 cryostat (Oxford Instruments). In a typical experiment instrument settings were: modulation frequency, 100 kHz; modulation amplitude, 0.5 Gauss; receiver gain, 6.2×10^2; microwave power, 10 mW. Variable-temperature magnetic measurements were performed in the temperature range 2.5–270 K using a Metronique Ingegnierie SQUID apparatus.

Electrochemical measurements were performed with an EG&G Princeton Applied Research (PAR) potentiostat/galvanostat, Model 273, or with an AMEL 5000 System, in conjunction with a Linseis X-Y recorder; for all readings a three-electrode system in CH$_2$Cl$_2$ containing 0.1 M of supporting electrolyte was employed. Cyclic voltammetric measurements were obtained with a double platinum electrode and a Ag–AgCl reference electrode equipped with a Luggin capillary under an atmosphere of purified N$_2$.

Synthesis

H$_2$oespz. The free-base porphyrazine [H$_2$oespz)] was synthesized according to the procedure reported earlier.[1,2] The product was carefully purified by flash chromatography on silica gel (first band) using a 1 : 1 CH$_2$Cl$_2$–hexane mixture as eluent (Found: C, 48.25; H, 5.27; N, 14.01; S, 32.15. C$_{32}$H$_{42}$N$_8$S$_8$ requires C, 48.33; H, 5.32; N, 14.09; S, 32.26%). ^{1}H NMR: δ_H(300 MHz, CDCl$_3$) -0.95 (2 H), 1.52 (24 H, t), 4.25 (24 H, q); UV/VIS (CH$_2$Cl$_2$): λ/nm (log ε) 360 (4.67) (Soret); 490 (4.17); 520 (4.18); 632 (4.58), 670 (sh) (4.56), 655 (4.60), 715 (4.81) (Q bands). FAB-MS (NBA matrix, positive ion mode): m/z 794, cluster, M^+ (calc. 794).

[Mn(oespz)]. The complex was prepared as previously reported.[1,2] In an inert atmosphere glove box reaction of H$_2$oespz (0.100 g, 0.13 mmol) with [Mn(O$_2$CMe)$_2$] (0.035 g, 0.20 mmol) in refluxing dry EtOH (10.0 cm^3) led, in 24 h, to a dark

blue solution that, after freezing at -70 °C overnight, filtration and washing with hexane, afforded metallic needle-like crystals of [Mn(oespz)] (yield $\approx 70\%$) (Found: C, 45.49; H, 4.37; N, 13.55; S, 30.17. C$_{32}$H$_{40}$N$_8$MnS$_8$ requires C, 45.31; H, 4.75; N, 13.21; S, 30.24%). UV/VIS (EtOH): λ/nm (log ε) 280 (4.28); 345 (4.37) (Soret); 420 (3.96), 450 (3.92); 590 (4.40), 640 (4.18), 720 (4.09) (Q bands).

[Mn(oespz)(SH)]. All reactions and manipulations were performed under an inert atmosphere. The complex [Mn(oespz)] (0.10 g, 0.12 mmol) was dissolved at 20 °C in freshly purified CS$_2$ (20.0 cm^3) under vigorous stirring. The solution immediately turned red. After 1 h, anhydrous THF (5.0 cm^3) was added dropwise to the solution and some small crystals started to form. The mixture was allowed to stand at 4.0 °C for 48 h. The precipitate was collected by filtration, washed with hexane and recrystallised from CS$_2$–hexane (yield > 90%) (Found: C, 44.00; H, 4.43; N, 12.76. C$_{32}$H$_{41}$N$_8$MnS$_9$ requires C, 43.61; H, 4.69; N, 12.71%). UV/VIS (C$_6$H$_6$): λ/nm (log ε) 337 (4.35); 418 (4.23) (Soret); 522 (4.27), 571 (4.22); 718 (4.33) (Q bands).

Crystallography

Crystal data, details of data collection and refinement parameters for [Mn(oespz)(SH)] are given in Table 1 and selected bond lengths and angles are given in Table 2. All data were collected at room temperature on an Enraf-Nonius CAD-4 diffractometer using graphite-monochromatized Cu-Kα radiation. The unit cell was determined from 25 well-centered reflections. The intensity data were collected in an ω–2θ scan mode. A total of 7474 reflections were measured to $\theta_{max} = 69°$; 3631 reflections with $I > 3\sigma(I)$ were used. Data reduction

included correction for background and Lorentz-polarizations effects. An absorption correction was applied according to ref. 14. The intensities of two reflections were measured every hour during data collection as a check of the stability of the diffractometer and the crystal; no appreciable decay of the intensities was observed. The crystal orientation was checked every 200 intensity measurements using two control reflections.

Structure analysis and refinement. The structure of [Mn-(oespz)(SH)] was solved by means of direct methods using MULTAN.[15] The analysis of the E-map derived from the set of phases with the best combined figure of merit revealed the position of most of the non-hydrogen atoms. In both cases the remaining atoms were located from successive Fourier syntheses. The structures were anisotropically refined by full-matrix least-squares procedures to an R value of 0.051 ($R' = 0.053$). The minimized function was $\Sigma w(|F_o| - |F_c|)^2$, with $w = 1$ for all the observed $I > 3\sigma(I)$ reflections. Hydrogen atoms, included in the structural model in stereochemically calculated positions, were refined but restrained to ride on the atoms to which they are bonded. The relatively large value of Δ/σ maxima are due to the presence of the C(22) carbon atom which shows unresolved disorder.

Atomic scattering factors and anomalous dispersion corrections were taken from ref. 16. All the computations were performed by the MOLEN package[17] running on a DEC VAX 6510 computer.

CCDC reference number 186/993.

Results and Discussion

Preparation and properties of [Mn(oespz)(SH)]

The formation of [Mn(oespz)(SH)] occurs in two steps: (*i*) reaction of [Mn^{II}(oespz)] with CS$_2$ to give an unstable adduct, (*ii*) reaction of this adduct with THF. The reaction of [Mn^{II}-(oespz)], a complex with a highly nucleophilic metallic center, and CS$_2$, is fast. On mixing, the solution of the manganese complex and carbon disulfide immediately turns from blue to red. The reaction consists of an oxidative addition of CS$_2$ to the manganese(II) center, leading, through equilibrium (1), to the

$$[Mn^{II}(oespz)] + CS_2 \rightleftharpoons [Mn^{III}(oespz)^+(CS_2)^{\cdot-}] \quad (1)$$
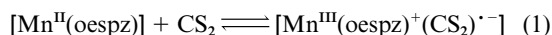
adduct [Mn^{III}(oespz)$^+$(CS$_2$)$^{\cdot-}$]. Oxidative addition of the Cl$^\cdot$ radical to the manganese(II) center was invoked to explain the easy C–Cl bond cleavage upon reaction of [Mn(oespz)] with chlorinated hydrocarbons.[2,3]

The formation of the adduct [Mn^{III}(oespz)$^+$(CS$_2$)$^{\cdot-}$] in CS$_2$ can be justified on the basis of experimental evidence, whereas its structure can be tentatively predicted on the basis of theoretical arguments. Indeed, we have found that removal of excess CS$_2$ from the reaction mixture by a N$_2$ stream leads to the recovery of the manganese(II) complex. It can be concluded, therefore, that the reaction simply involves the abstraction of a sulfur atom from CS$_2$. The UV/VIS spectrum of the proposed adduct [Mn^{III}(oespz)$^+$(CS$_2$)$^{\cdot-}$] shows typical absorptions of a manganese(III) porphyrazine,[2] and significantly differs from that of [Mn^{III}(oespz)(SH)] in CS$_2$. The Soret and the Q band of [Mn^{III}(oespz)(SH)] lie, in CS$_2$, at 340 and 705 nm, respectively, whereas these bands occur at 350 and 726 nm in the case of the adduct.

As for the structure of [Mn^{III}(oespz)$^+$(CS$_2$)$^{\cdot-}$] a η^1-C arrangement (**a**) (see below) seems rather unlikely, on the basis of steric arguments. Although, in fact, the $a_{2u}(\pi^*)$ LUMO orbital of a linear (D_h) CS$_2$ molecule (this orbital becomes a_1 for a slightly bent CS$_2$ molecule with C_{2v} symmetry)[18,19] which becomes semi-occupied upon reaction with [Mn(oespz)] is largely localized on the carbon atom, a η^1-C structure would lead to severe CS$_2$–macrocycle repulsive interactions. Similar

arguments might hold, in part, for a η^2-C,S arrangement (**b**), leaving a η^1-S structure (**c**) of the adduct as the most likely. Unlike the η^2-C,S, co-ordination mode, however, the η^1-S co-ordination mode of CS$_2$ has not been characterized and has been only proposed for a few organometallic compounds.[4] This co-ordination mode is predicted, in fact, based on electronic structure considerations, to lead to highly unstable systems. A structure in between **b** and **c** seems more appropriate in interpreting the last step of the reaction, and would involve either H or H$^\cdot$ radical abstraction from THF by the highly reactive [Mn^{III}(oespz)$^+$(CS$_2$)$^{\cdot-}$] leading to C–S bond cleavage and to the formation of CS$^+$ or CS and [Mn(oespz)(SH)]. Carbon–sulfur bond cleavage in η^2- bound CS$_2$ and related ligands is a facile process and is observed,[20] for instance, in the insertion of the chalcogen atom of COS into a metal–hydride bond. On the other hand, formation of hydrogensulfide ligands from metal sulfides and hydrogen has been also reported.[21]

a   b   c
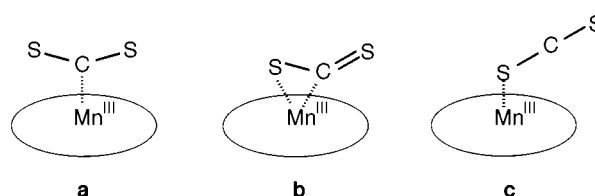
Interestingly, the compound [Mn(oespz)(SH)] can be also obtained by the reaction of [Mn(oespz)] with a saturated ethanolic solution of H$_2$S. Besides the [Mn(oespz)(SH)] complex, the reaction leads to production of H$_2$. As inferred from the gas-chromatographic quantitative analysis[22] of the evolved H$_2$, the stoichiometry of this reaction agrees with equation (2).

$$2[Mn^{II}(oespz)] + 2H_2S = 2[Mn^{III}(oespz)(SH)] + H_2 \quad (2)$$

A detailed description of the mechanistic aspects of this reaction will be presented elsewhere.[23]

Unlike [Fe(TAP)(SH)] [TAP = 5,10,15,20-tetrakis(*p*-methoxyphenyl)porphyrinato dianion], [Mn(oespz)(SH)] is not very oxygen sensitive in solution and we did not find evidence for the formation of the μ-oxo dimer, as in the case of the iron complex, upon exposure to dry oxygen.[8a] The Mn^{III} ⟶ Mn^{II} process occurs reversibly ($i_{pa}/i_{pc} = 1$, $\Delta E_p = 60$ mV, where i_{pa} and i_{pc} are, respectively, the anodic peak current and the cathodic peak current) at $E_{\frac{1}{2}} = 0.178(5)$ V (*vs.* Ag–AgCl). This value is, similar to that found in [Mn(oespz)Cl], considerably anodically shifted relative to manganese porphyrins and might be an origin of the unusual stability of this complex.[2] That this value is only slightly more anodic than in [Mn(oespz)Cl] confirms the observed tendency of porphyrazines to stabilize the low oxidation states of first-row transition metals.[1,2] This also indicates that axial ligands of different σ-donor capability, but with scarce π-acceptor capability,[24] only marginally influence the Mn^{III}–Mn^{II} redox process in manganese tetraazaporphyrins.

In the IR spectrum of [Mn(oespz)(SH)], taken as a CCl$_4$ solution or as KBr pellets, no bands due to S–H vibration are seen, as hydrogensulfide stretches in metal complexes are generally weak and often not observed.[7a,25] The near-IR spectrum of a thin film of the complex is shown in Fig. 1. It is, in the higher energy region, qualitatively similar to that observed for chloromanganese(III) porphyrazine in solution. Moreover the spectrum reveals rather intense bands in the ranges 1300–1800 and 2300–2800 nm, that are not present in the solution spectrum. In order to check if these signals are caused by S–H vibrations or to electronic transitions, we recorded a near-IR spectrum of a hydrosulfido compound (2-naphthalenethiol). Since the thin film near-IR spectrum of 2-naphthalenethiol did not show significant absorptions in the ranges 1300–1800 and 2300–2800 nm, it appears plausible that the lowest lying bands in the near-
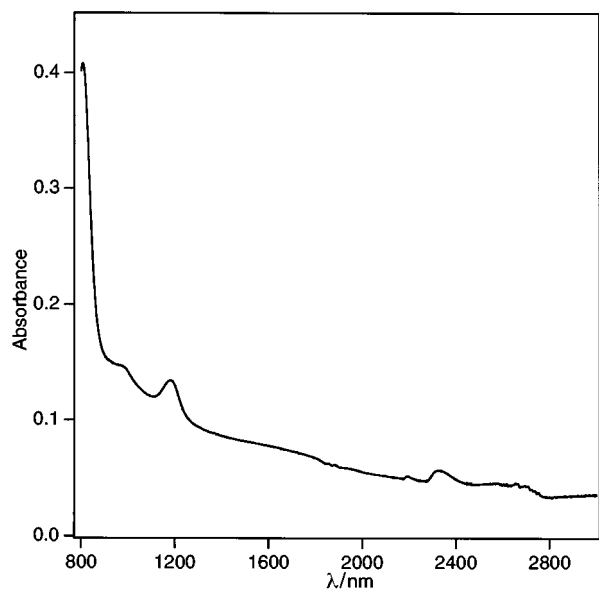
Fig. 1 Near-IR absorption spectrum of a thin film of [Mn(oespz)-(SH)] deposited on a quartz slide

IR spectra of the complex are due to lattice intermolecular interactions rather than to S–H vibrations.

The room-temperature ^{1}H NMR spectrum of [Mn(oespz)-(SH)] taken in CD$_3$OD, instead, reveals a broad peak at δ 10.3 ascribed, on integration, to the hydrogensulfide proton resonance. The ^{1}H NMR resonance of this proton occurs at δ −1.21 in CDCl$_3$ for [Rh(SH)(CO)(PPh$_3$)$_2$][7a] and at δ −18.4 for [RhCl(H)(μ-SH)(PPh$_3$)$_2$]$_2$·2CH$_2$Cl$_2$,[7b] indicative of the large sensitivity of the hydrogensulfide proton resonance to the nature of the metal and the other ligands. Nevertheless the ^{1}H NMR resonance of the sulfur-bound proton in [Mn(oespz)-(SH)] compares well with that of [Fe(TAP)(SH)] occurring at δ 6.75.[8a] It can be concluded that the ^{1}H NMR signal at δ 10.3 in [Mn(oespz)(SH)] is due to a proton bound to a pyrrolic nitrogen. Infrared spectra in CCl$_4$ did not show any evidence of N–H bond stretching in the region 3000–3400 cm^{-1}. Based on these data, the possible interchange of the hydrogensulfide proton between the apical sulfur and a pyrrolic nitrogen also appears to be quite unlikely (see below).
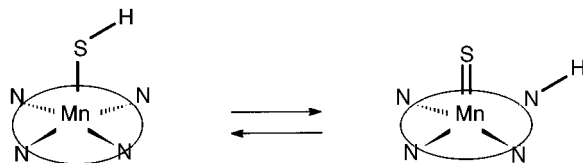
Description of the crystal structure

The complex [Mn(oespz)(SH)] is isostructural with [Mn-(oespz)Cl] and [Fe(oespz)Cl][2] and, for this reason, its structure will be briefly described. Fig. 2 is a computer-drawn model of the [Mn(oespz)(SH)] molecules as it exists in the crystal. The co-ordination geometry around the manganese atom is that of a slightly distorted square pyramid. The displacement of the metal atom out of the planar (N$_p$)$_4$ (N$_p$ = pyrrolic nitrogen atoms) donor set is 0.294(1) Å. Thus the MN$_4$ group is only slightly more pyramidal than in [Mn(oespz)Cl][2] and in [Mn-(tpp)Cl][27] (H$_2$tpp = *meso*-5,10,15,20-tetraphenylporphyrin).[27] We notice that the Fe out-of-plane distance is 0.33 Å in the parent, low-spin ($S = \frac{1}{2}$) [Fe(TAP)(SH)] complex.[8a] The average Mn–N$_p$ distance is 1.946(5) Å, a value comparable to that in [Mn-(oespz)Cl] [1.951(6) Å] and in the Mn^{III}–phthalocyaninato μ-oxo dimer, [Mn$_2$(pc)$_2$(py)$_2$O] [1.960(3) Å], but shorter than in [Mn(tpp)(Cl)] [2.082(2) Å].[2,19,20]

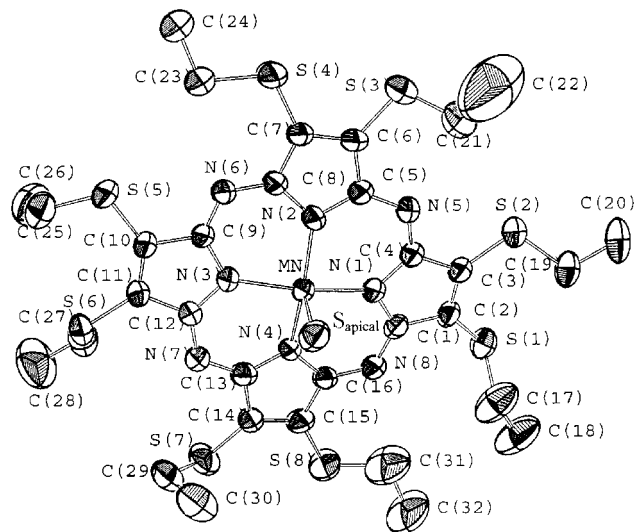That the Mn–N$_p$ distance is shorter than in [Mn(tpp)(Cl)]

and the extent of MnN$_4$ pyramidalization are consistent with the remarkable contraction of the co-ordinating cavity in the porphyrazines and with the presence of an unoccupied antibonding d$_{x^2-y^2}$ orbital. It should be considered, however, that a contribution to the pyramidalization arises from the necessity to minimize non-bonded contacts between the hydrosulfido axial ligand and the (N$_p$)$_4$ core atoms. The Mn–S$_{apical}$ distance of 2.374(3) Å is in the range expected for this bond in transition-metal hydrosulfido complexes. Actually, M–S distances of 2.298(3), 2.418(3) and 2.340(2) Å respectively have been found in [Fe(TAP)(SH)], *trans*-[Rh(SH)(CO)(PPh$_3$)$_2$] and *cis*-[Pt(SH)$_2$(PPh$_3$)$_2$].[7a,8a,28] On the other hand, M–S distances ranging from 2.395(3) to 2.591(5) Å are found in manganese(II) complexes containing thiolate ligands.[29] For the tetraazaporphyrinato core, the dimensional variations in bond length and angles of chemically analogous bond types differ immaterially from four-fold geometry. However, as previously noted in other structurally characterized porphyrazines, the C$_\beta$–C$_\beta$ bonds are significantly contracted with respect to [M(pc)] complexes [average bond lengths of 1.365(5) *vs.* 1.395(5) Å].[1] The crystal packing of [Mn(oespz)(SH)] consists of slipped stacks of dimeric units. The monomers are slipped within each dimer, positioned in a *trans* fashion with respect to the Mn–S$_{apical}$ bond and weakly associated *via* long contacts between the Mn and S(1) atoms of the adjacent molecule [Mn···S(1) 3.250(3) Å]. Intradimer interactions at the van der Waals limit also occur between the N(3) and N(4) atoms and the S(1) atom of the adjacent molecule: N(3)···S(1) 3.262(7), N(4)···S(1) 3.285(7) Å. Owing to the peculiar structure of the dimer, the repulsion between the N(3) and N(4) out-of-plane lone pairs and the S(1) lone pair, prevents a closer Mn···S(1) approach. Along the stack weak interdimer interactions [3.612(2) Å] arise from S(5)···S$_{apical}$ contacts [S(5) at $-x, \frac{1}{2} + y, \frac{1}{2} - z$].

EPR and magnetic susceptibility data

The nature and the strength of the intradimer interactions account for the solid-state magnetic behaviour of [Mn(oespz)-(SH)]. The temperature dependence of the magnetic susceptibility, χ *versus* T, measured in the temperature range 3.5–240 K is shown in Fig. 3. The high temperature effective magnetic moment, μ$_{eff}$ = $8kT$ = 6.8 μ$_B$ which compares well with the spin-only value expected for two $S = 2$ non-interacting spins (μ$_{eff}$ = 6.9 μ$_B$). The χ *versus* T curve shows a clear maximum around 5 K indicating that an antiferromagnetic interaction is operative between the two spin centers. The compound was found to be EPR silent down to 4.3 K, as expected for a
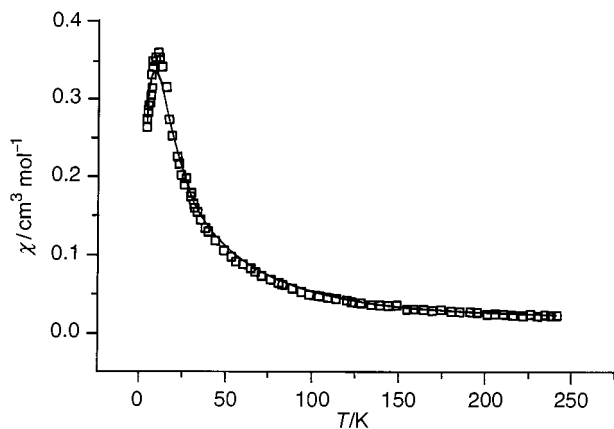
Fig. 3 Temperature dependence of the magnetic susceptibility of [Mn(oespz)(SH)]. The solid line is the best fit curve
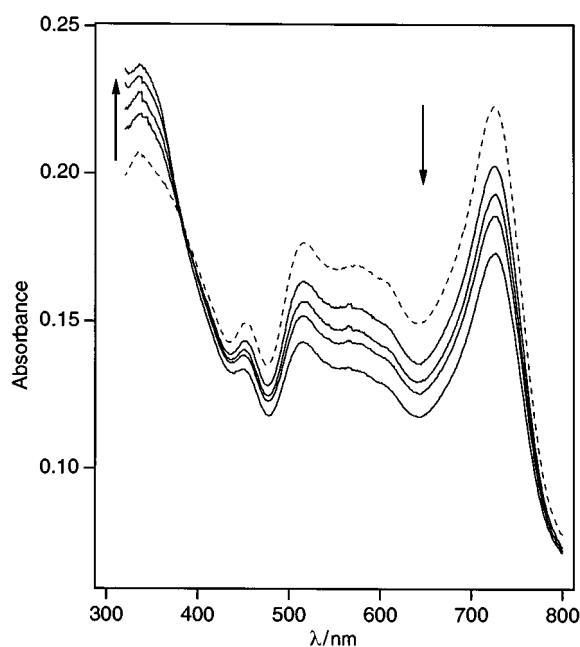

Fig. 4 Spectroscopic titration of [Mn(oespz)(SH)] (– – –) with 2,4,6-trimethylpyridine in chloroform at 20 ± 0.1 °C. $[Mn]_{tot} = 1.02 \times 10^{-5}$ M, [2,4,6-trimethylpyridine] = 0–0.05 M

non-Kramers spin system.[30] Using the isotropic exchange hamiltonian in the form $H = JS_1 \cdot S_2$ to describe the magnetic interaction, the equation describing the temperature dependence of the magnetization takes the form (3).

$$\chi = \frac{Ng^2\mu_B^2}{kT} \frac{2e^{-J/kT} + 10e^{-3J/kT} + 28e^{-J/kT} + 60e^{-10J/kT}}{1 + 3e^{-J/kT} + 5e^{-3J/kT} + 7e^{-6J/kT} + 9e^{-10J/kT}} \quad (3)$$

The magnetic data have been fitted by minimizing function (4) where χ_j^o and χ_j^c are the observed and the computed values at

$$F = \sum_j (\chi_j^o - \chi_j^c)^2 \quad (4)$$

temperature T_j, using a Simplex minimization routine.[31] The best fit curve, obtained with $g = 1.99(2)$ and $J = 1.90(6)$ cm^{-1}, is shown in Fig. 3 as a solid line.

Co-ordination chemistry of [Mn(oespz)(SH)]

In order to elucidate the structure of the complex in solution and the possible effects of the sixth ligand on the electronic structure of the complex, we studied the co-ordinating capability of the complex towards strong σ-donors such as 1-mim as well as towards sterically hindered organic bases such as 2,4,6-
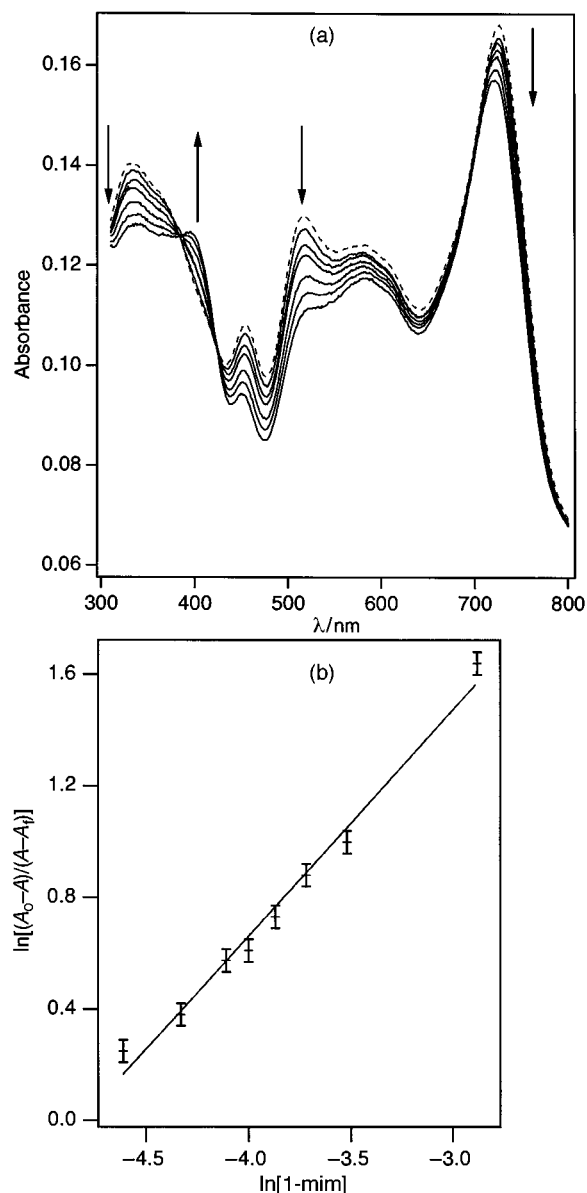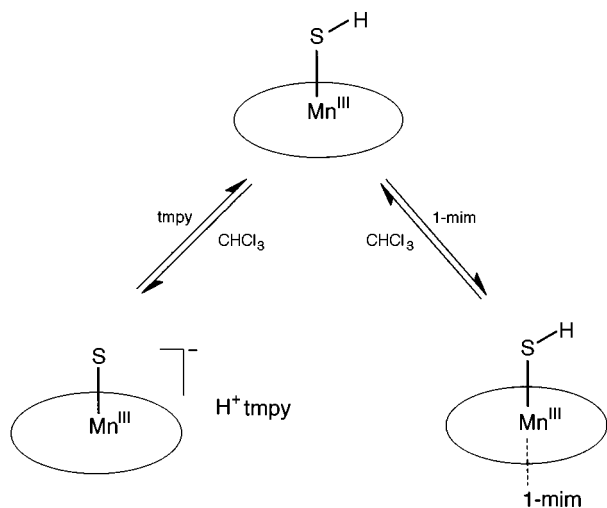

Fig. 5 (a) Spectroscopic titration of [Mn(oespz)(SH)] (– – –) with 1-mim in chloroform at 20 ± 0.1 °C. $[Mn]_{tot} = 1.02 \times 10^{-5}$ M, [1-mim] = 0–0.17 M. (b) Plot of $\ln[(A_0 - A)/(A - A_f)]$ as a function of $\ln[1\text{-mim}]$ as monitored by the decrease of the absorbance maximum at 718 nm

trimethylpyridine. Treatment, at 20.0 ± 0.1 °C, of a chloroform solution of [Mn(oespz)(SH)] (1.0×10^{-5} M) with aliquots of a solution of 2,4,6-trimethylpyridine (tmpy) in chloroform, leads to an isosbestic change in the visible spectrum, as shown in Fig. 4. At relatively high concentrations of 2,4,6-trimethylpyridine (0.05 M) a limiting spectrum, indicative of saturation is obtained.

The spectra were analyzed by plotting $\ln[(A_0 - A)/(A - A_f)]$ *versus* $\ln[2,4,6\text{-methylpyridine}]$ at 320 and 725 nm.[31,32] The two plots were linear with an average slope of 1.0 ± 0.1 indicating the formation of the [Mn(oespz)S$^-$][H$^+$tmpy] adduct.

The changes in the electronic spectra of a chloroform solution of [Mn(oespz)(SH)] upon progressive addition of a 1-methylimidazole–chloroform solution at the same temperature are displayed in Fig. 5(a). Addition of a strong σ-donor, sterically unhindered base, is accompanied by a marked increase of the absorbance at 417 nm, a decrease at 450 and at 718 nm leading to isosbestic points at 370 and 435 nm. At relatively high concentration of 1-mim a limiting spectrum is obtained. In the plots of $\ln[(A_0 - A)/(A - A_f)]$ *versus* $\ln[1\text{-mim}]$ at 725 nm the data lie on a single straight line of average slope 1.0 ± 0.1 indicating the formation of the 1:1 six-co-ordinated [Mn(oespz)-
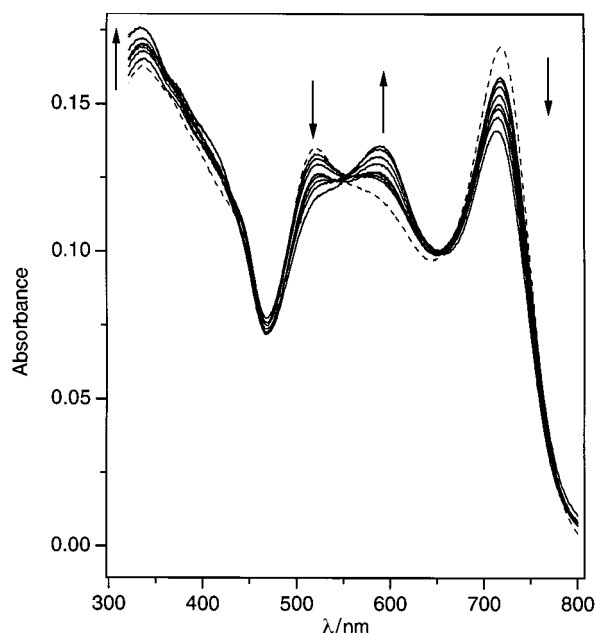
Scheme 1

Fig. 6 Spectroscopic titration of [Mn(oespz)(SH)] (– – –) with 1-mim in benzene at 20 ± 0.1 °C. $[Mn]_{tot} = 0.76 \times 10^{-5}$ M, [1-mim] = 0–0.17 M

(SH)(1-mim)] complex [see Fig. 5(b)]. It is remarkable that the spectroscopic changes noted upon addition of 1-mim are qualitatively similar to those observed when [Mn(oespz)X] (X = halogen) are titrated with the same base in chloroform.[3] These results support the conclusion that, contrary to 2,4,6-trimethylpyridine, the 1-mim attack occurs on the manganese atom rather than on the hydrosulfido axial ligand and confirm, *de facto*, the presence of an apical S–H group (see Scheme 1) in the complex.

Notably, on dilution, the main spectral features of pure [Mn(oespz)(SH)] are restored. Thus the processes earlier described are reversible and the effect of dilution can be understood in light of the fact that it acts, most likely, on the saturation conditions.

Upon treatment of a diluted benzene solution of [Mn(oespz)-(SH)] with aliquots of solutions of 1-mim in the same solvent, the spectral changes indicate that the co-ordination of the organic base to manganese is accompanied by a redox process, and a saturation concentration of 1-mim is not reached (Fig. 6). Actually the spectra become progressively similar to that of [Mn(oespz)] indicating that a $Mn^{III} \longrightarrow Mn^{II}$ process is occurring.[1] As a matter of fact, the intensity of the Q band at 590 nm progressively increases whereas, concomitantly, that of the band at 720 nm decreases. It was recently demonstrated that

the occurrence of an intense band at 590 nm is diagnostic of the Mn^{II} systems in the manganese porphyrazines.[2]

These results clearly indicate that the dimerization of the complex is a solid-state process and that in solution the $Mn \cdots S$ intermolecular interactions no longer exist or, at least, can be easily replaced by interactions of the metal with a ligand having stronger σ-donor capability than that of the sulfanyl function. Co-ordination of the sixth ligand induces important changes in the spectrum of the complex, especially in the region 350–500 nm where ligand-to-metal charge transfer (LMCT) transitions are normally found in redox-active transition-metal porphyrazines.[1,2] Depending on the solvent, additional redox processes involving the metal may occur as well. Thus the electrochemical stability and the rich co-ordination chemistry of this complex may stimulate further studies on related complexes to understand the spectroelectrochemical behavior of tetrapyrrole systems of biological interest.

In the presence of 2,4,6-trimethylpyridine the axial SH transforms into an out-of-plane thiolate co-ordinating site. Polynuclear complexes of gold(I) or mercury(II) which easily co-ordinate the thiolate ligand, can be built up exploiting this important feature of the complex.[33] These possibilities are currently being explored in our laboratory.

Conclusion

Oxidative addition of CS_2 to [Mn(oespz)] affords the [Mn-(oespz)(SH)] complex that has been characterized by conventional spectroscopies and by cyclic voltammetry. The crystal structure of the complex, that represents the second case of a porphyrin-like complex with a hydrosulfido axial ligand that has been structurally characterized, does not differ significantly from that of similar manganese(III) porphyrazines. The high spin ($S = 2$) ground state is consistent with the geometry of the MnN_4 core and the weak antiferromagnetic coupling $[J = 1.90(6)$ cm$^{-1}]$ between magnetic centers within [Mn(oespz)-(SH)]$_2$ dimers. In CHCl$_3$ [Mn(oespz)(SH)] reacts reversibly with the sterically hindered base 2,4,6-trimethylpyridine through the axial hydrosulfido ligand, whereas the complex co-ordinates reversibly 1-mim on the vacant site of manganese. Treatment of the complex with 1-mim in benzene leads to a $Mn^{III} \longrightarrow Mn^{II}$ redox process, as deduced from the UV/VIS spectra.

Acknowledgements

References

1 G. Ricciardi, A. Bencini, A. Bavoso, A. Rosa and F. Lelj, *J. Chem. Soc., Dalton Trans.*, 1996, 3243.
2 G. Ricciardi, A. Bavoso, A. Bencini, A. Rosa, F. Lelj and F. Bonosi, *J. Chem. Soc., Dalton Trans.*, 1996, 2799.
3 G. Ricciardi, S. Belviso, K. Pilat and F. Lelj, unpublished work.
4 C. Bianchini, C. Mealli, A. Meli and M. Sabat, *Stereochemistry of Organometallic and Inorganic Compounds*, ed. I. Bernal, Elsevier, Amsterdam, 1986, vol 1, p. 146.
5 G. Steimecke, R. Kirmse and E. Hoyer, *Z. Chem.*, 1975, **15**, 28.
6 E. Hoyer, *Comments Inorg. Chem.*, 1983, **2**, 261.
7 (*a*) T. R. Gaffney and J. A. Ibers, *Inorg. Chem.*, 1982, **21**, 2857; (*b*) A. M. Mueting, P. Boyle and L. H. Pignolet, *Inorg. Chem.*, 1984, **23**, 44; (*c*) T. B. Rauchfuss and C. Ruffling, *Organometallics*, 1982, **1**, 400.
8 (*a*) D. R. English, D. N. Hendrickson, K. S. Suslick, C. W.

Eigenbrot, jun. and W. R. Scheidt, *J. Am. Chem. Soc.*, 1984, **106**, 7258; (*b*) J. H. Dawson, J. R. Trudell, G. Barth, R. E. Linder, E. Bunnenberg, C. Djerassi, R. Chiang and L. P. Hager, *J. Am. Chem. Soc.*, 1976, **98**, 3709; (*c*) S. W. McCann, F. V. Wells, H. H. Wickmann, T. N. Sorrell and J. P. Collman, *Inorg. Chem.*, 1980, **19**, 621.

9 I. Fridovich, *Annu. Rev. Biochem.*, 1995, **64**, 97.
10 G. C. Dismukes, *Chem. Rev.*, 1996, **96**, 2909.
11 J. S. Miller, J. C. Calabrese, R. S. McLean and A. J. Epstein, *Adv. Mater.*, 1992, **4**, 498.
12 J. S. Miller, C. Vasquez, J. C. Calabrese, R. S. McLean and A. J. Epstein, *Adv. Mater.*, 1994, **6**, 217.
13 D. D. Perrin and W. L. F. Armarego, *Purification of laboratory chemicals*, Pergamon Press, Oxford, 3rd edn., 1988.
14 N. Walker and D. Stuart, *Acta Crystallogr., Sect. A*, 1983, **39**, 159.
15 MULTAN 82, Structure determination package, B. A. Frentz and Associates, College Station, TX, 1982.
16 *International Tables for X-Ray Crystallography*, Kynoch Press, Birmingham, 1974, vol. IV, p. 99.
17 C. K. Fair, MOLEN, Structure Determination System, Delft, The Netherlands, 1990.
18 R. S. Alvarez, R. Vicente and R. Hoffmann, *J. Am. Chem. Soc.*, 1985, **107**, 6253.
19 C. Mealli, R. Hoffmann and A. Stockis, *Inorg. Chem.*, 1984, **23**, 56.
20 H. L. M. van Gaal and J. P. J. Verlaan, *J. Organomet. Chem.*, 1977, **133**, 93; H. Werner and O. Kolb, *Angew. Chem., Int. Ed. Engl.*, 1979, **18**, 865; T. R. Gaffney and J. A. Ibers, *Inorg. Chem.*, 1982, **21**, 2851.
21 M. Rakowski DuBois, M. C. Van Derveer, D. L. DuBois, R. C. Haltiwanger and W. K. Miller, *J. Am. Chem. Soc.*, 1980, **102**, 7456.
22 R. Henning, W. Schlamann and K. Kisch, *Angew. Chem., Int. Ed. Engl.*, 1980, **19**, 645.
23 G. Ricciardi, S. Belviso and F. Lelj, unpublished work.
24 G. M. Brown, F. R. Hopf, T. J. Meyer and D. G. Whitten, *J. Am. Chem. Soc.*, 1975, **97**, 5385; F. A. Walker, D. Beroiz and K. M. Kadish, *J. Am. Chem. Soc.*, 1976, **98**, 3484.
25 J. P. Collman, R. K. Rothrock and R. A. Stark, *Inorg. Chem.*, 1977, **16**, 437.
26 C. K. Johnson, ORTEP, Report ORNL-5138, Oak Ridge National Laboratory, Oak Ridge, TN, 1976.
27 L. H. Vogt, A. Zalkin and D. H. Templeton, *Inorg. Chem.*, 1967, **6**, 1725.
28 C. E. Briant, G. R. Hughes, P. C. Minshall and D. M. P. Mingos, *J. Organomet. Chem.*, 1980, **202**, C18.
29 H. O. Stephan and G. Henkel, *Polyhedron*, 1996, **15**, 501; J. A. Castro, J. Romero, J. A. Garcia-Vazquez, A. Castineiras, A. Sousa and J. Zubieta, *Polyhedron*, 1995, **14**, 2841; B. Krebs and G. Henkel, *Angew. Chem., Int. Ed. Engl.*, 1991, **30**, 769; A. Silver, S. A. Koch and M. Millar, *Inorg. Chim. Acta*, 1993, **205**, 9.
30 A. Abragam and B. Bleaney, *Electron paramagnetic resonance of transition ions*, Oxford Press, Oxford, 1970.
31 C. J. O'Connor, *Prog. Inorg. Chem.*, 1982, **29**, 203.
32 H. Jaffé and M. Orchin, *Theory and Applications of Ultraviolet Spectroscopy*, Wiley, New York, 1992, p. 578.
33 J. Fitzgerald, B. S. Haggerty, A. N. Rheingold and L. May, *Inorg. Chem.*, 1992, **31**, 2006.
34 J. M. Foward, D. Bohmann, J. P. Falcker, jun. and R. J. Staples, *Inorg. Chem.*, 1995, 6330.